Applying ANN, ANFIS and LSSVM Models for Estimation of Acid Solvent Solubility in Supercritical CO_2

**Amin Bemani[1], Alireza Baghban[2], Shahaboddin Shamshirband[3, 4, *],
Amir Mosavi[5, 6, 7], Peter Csiba[7] and Annamaria R. Varkonyi-Koczy[5, 7]**

Abstract: In the present work, a novel machine learning computational investigation is carried out to accurately predict the solubility of different acids in supercritical carbon dioxide. Four different machine learning algorithms of radial basis function, multi-layer perceptron (MLP), artificial neural networks (ANN), least squares support vector machine (LSSVM) and adaptive neuro-fuzzy inference system (ANFIS) are used to model the solubility of different acids in carbon dioxide based on the temperature, pressure, hydrogen number, carbon number, molecular weight, and the dissociation constant of acid. To evaluate the proposed models, different graphical and statistical analyses, along with novel sensitivity analysis, are carried out. The present study proposes an efficient tool for acid solubility estimation in supercritical carbon dioxide, which can be highly beneficial for engineers and chemists to predict operational conditions in industries.

Keywords: Supercritical carbon dioxide, machine learning, acid, artificial intelligence, solubility, artificial neural networks (ANN), adaptive neuro-fuzzy inference system (ANFIS), least-squares support vector machine (LSSVM), multilayer perceptron (MLP).

1 Introduction

In recent years, supercritical fluid has become one of the interests of chemical engineers and chemists as a novel and extensive applicable technology. The synthesis and generating of nanomaterials and extraction process of different materials are the popular applications of supercritical fluids [Inomata, Honma, Imahori et al. (1999); Stassi and Bettini (2000);

---

[1] Petroleum Engineering Department, Petroleum University of Technology, Ahwaz, Iran.

[2] Chemical Engineering Department, Amirkabir University of Technology, Mahshahr Campus, Mahshahr, Iran.

[3] Department for Management of Science and Technology Development, Ton Duc Thang University, Ho Chi Minh, Vietnam.

[4] Faculty of Information Technology, Ton Duc Thang University, Ho Chi Minh, Vietnam.

[5] Kalman Kando Faculty of Electrical Engineering, Obuda University, Budapest, 1034, Hungary.

[6] Institute of Structural Mechanics, Bauhaus University Weimar, Weimar, D-99423, Germany.

[7] Department of Mathematics and Informatics, J. Selye University, Komarno, 94501, Slovakia.

*Corresponding Author: Shahaboddin Shamshirband. Email: shahaboddin.shamshirband@tdtu.edu.vn.

Ohde, Hunt and Wai (2001); Celso, Triolo and Mcclain (2002); Uzer, Akman and Sarker (2006); Munshi and Bhaduri (2009); Nahar and Sarker (2012); Zhang, Heinonen and Levanen (2014); Knez and Cor (2017); Zhao, Zhang, Zhao et al. (2017); Belghait, Si-Moussa, Laidi et al. (2018); Gao, Daryasafar, Lavasani et al. (2018)]. One of the supercritical fluids which have wide applications in the extraction of various metals from solid and liquid phases is carbon dioxide [Erkey (2000); Sunarso and Ismadji (2009); Lin, Liu, Maiti et al. (2014)]. Due to non-flammability, nontoxicity, low cost, and critical points (304.2 K and 7.38 MPa) of carbon dioxide, the supercritical carbon dioxide becomes one of the interesting and applicable supercritical fluids in industries [Ghaziaskar and Nikravesh (2003); Bovard, Abdi, Nikou et al. (2017)]. The viscosity and density of supercritical carbon dioxide are known as two important transport properties of the fluids which are affected by pressure and temperature [Choubin, Abdolshahnejad and Moradi (2020); Shamshirband, Hadipoor and Baghban (2019)]. Another dominant thermos physical property of supercritical carbon dioxide is the solubility of different materials in supercritical carbon dioxide which is a function of various factors such as polarity, molecular weight, pressure, temperature, and vapor pressure [Huang, Chiew, Lu et al. (2005); Ghaziaskar and Kaboudvand (2008)].

One types of the materials which have a solubility in supercritical carbon dioxide are acids, the nanofluoropentanoic acid which is known as one type of perfluorocarboxylic acids, has extensive applications in the production of paints additives, polymers, foams, and stain repellents but because of their high ability instability, they are harmful to environment [Richter and Dibble (1983); Moody and Field (1999); Hintzer, Löhr, killich et al. (2004); Fei and Olsen (2011); Hubbard, Guo, Krebs et al. (2012); Dartiguelongue, Leybros and Grandjean (2016); Hintzer, Juergens, Kaempf et al. (2016)]. Adrien Dartiguelongue and coworkers studied solubility of perfluoropentanoic acid in supercritical carbon dioxide in the wide range of temperature and pressure and also proposed some density-based models to predict solubility in terms of density of supercritical fluids [Dartiguelongue, Leybros and Grandjean (2016)]. Gurdial et al. [Gurdial and Foster (1991)] constructed dynamic setup to study solubility of o-, m- and p-hydroxybenzoic acid in the supercritical carbon dioxide in the wide range pressure of 80-205 mbar and temperature range of 308.15-328.15 K and correlated the measured solubility as a function of density. Kumoro measured the solubility of 2R,3β-dihydroxyurs-12-en-28-oic acid which is called Corosolic acid dynamically in a different range of pressure 8 to 30 MPa and five different temperatures of 308.15, 313.15, 323.15, and 333.15 K. Kumoro used various density-based models to correlate the experimental data [Kumoro (2011)].

Sahihi et al. [Sahihi, Ghaziaskar and Hajebrahimi (2010)] measured the solubility of Maleic acid in supercritical carbon dioxide by utilization of static experimental setup. The measured data belongs to Maleic acid in a pressure range of 7 to 300 bar and temperature of 348.15 K. Ghaziaskar and coworkers used a continuous flow set up to study solubility of tracetin, diacentin and acetic acid in supercritical carbon dioxide in the pressure range of 70 to 180 bar and various temperature of 313, 333 and 348 K and they also compared the obtained solubilities for different acids [Ghaziaskar, Afsari, Rezayat et al. (2017)]. Helena Sovova adjusted the Adachi-Lu equation based on the solubility of Ribes nigrum (blackcurrant) and Vitis vinifera (grape-vine) in supercritical carbon dioxide. They concluded the Adachi-Lu equation has enough accuracy in forecasting solubility of

triglycerides in carbon dioxide [Sovova, Zarevucka, Vacek et al. (2001)].

The issue of prediction of various acids solubility in supercritical carbon dioxide and phase equilibrium investigation of supercritical carbon dioxide and different materials are the important topics in chemical engineering research [Hemmati-Sarapardeh and Hajirezaie (2020)]. According to the hardships of experimental studies such as special tools and procedure which are needed, in the present work, the data-driven methods and advanced machine learning models have been considered as the reliable solutions, e.g., [Anitescu, Atroshchenko, Alajlan et al. (2019); Zarei, Razavi, Baghban et al. (2019); Mosavi, Shamshirband, Salwana et al. (2019); Mosavi, Salimi and Faizollahzadeh (2019); Najafi, Faizollahzadeh, Mosavi et al. (2018)]. In this paper four different algorithms, Radial basis function artificial neural network (RBF-ANN), Multi-layer Perceptron artificial neural network (MLP-ANN), Least squares support vector machine (LSSVM) and Adaptive neuro-fuzzy inference system (ANFIS) are developed to predict the solubility of different types of acid in supercritical carbon dioxide based on the various parameters such as structure of acid, pressure and temperature.

2 Methodology

2.1 Experimental data gathering

The dominant purpose of the present paper is the development of accurate and simple models to forecast solubility of different acids in supercritical carbon dioxide. Due to this, the required actual data for training and testing phases of models were assembled from the reliable source existed in literature [Gurdial and Foster (1991); Sovova, Zarevucka, Vacek et al. (2001); Sparks and Hernandez (2007); Tian, Jin, Gua et al. (2007); Sparks, Estevez, Hernandez et al. (2008); Kumoro (2011); Dartiguelongue, Leybros and Grandjean (2016)]. This collection of data contains the 188 acid solubility data points in terms of pressure, temperature, acid dissociation constant, molecular weight, number of carbon and hydrogen of acid. The details of data collection are reported in Tabs. S1 and S2. These details include acid name, acid dissociation constant, pressure and temperature ranges, and the number of utilized data points for each acid. Also, for clarification of this experimental dataset, the structure, linear formula and molecular weight of utilized acids are presented in Tab. S3. These acids include Perfluoropentanoic acid, o-Hydroxybenzoic Acid, Corosolic Acid, Maleic Acid, Ferulic Acid, Azelaic Acid, p-aminobanzoic acid, and Nonanioc acid.

2.2 Artificial neural networks

Artificial neural networks have amazing similarities to the performance and structure of neuron units in the brain system [Smith (1993); Bas and Boyaci (2007)]. These computational blocks construct different types of a layer such as input, output, and hidden layers. In the layers, there are transfer functions or activation function which organize the process of training in the algorithm. Each neuron has specific weight and bias values that control the optimization process. The artificial neural networks have the ability to trace a nonlinear form relationship between input and output parameters. Due to this ability, artificial neural networks have a widespread application in different industries and sciences. Artificial neural networks can be classified in different forms, such as a recurrent neural network (RNN), radial basis function, and multilayer perceptron [Movagharnejad and

Mehdizadeh (2011); Abdi-Khanghah, Bemani and Naserzadeh (2018); Zamen (2019)]. In the present work, the MLP and RBF network are utilized.

2.3 Least squares support vector machine

Vapnik [Vapnik (1998)] proposed the support vector machine based on statistical learning theory. This computational intelligence can be used for regression and classification purposes [Faizollahzadeh, Najafi, Alizamir et al. (2018); Riahi-Madvar and Dehghani (2019)]. However, there are many advantages to this method, but there is a hardship in its computational procedure because of quadratic programming. The least-squares SVM (LSSVM) is proposed as a novel type of SVM to solve this problem. This novel approach organized linear equations for computation and optimization [Cortes and Vapnik (1995); Suykens and Vandewalle (1999, 2001); Zamen (2019)].

By considering a dataset of $(x_i, y_i)_n$, the LSSVM regression prediction is utilized to estimate a function, where x_i and y_i are known as input and target parameters and n represent the number of data which utilized in training phase [Wang (2005)]. The linear regression is formulated, such as the following:

$$y = \omega^T \varphi(\text{x}) + \text{b} \tag{1}$$

where $\varphi(x)$ denotes a nonlinear function that has different forms such as polynomial, linear, sigmoid, and radial basis functions. Also, ω and b denote the weights and determined constant-coefficient in the training process. A new optimization problem can be defined based on LSSVM approach [Baghban, Bahadori, Lemraski et al. (2016); Baghban, Namvarrechi, Phung et al. (2016); Ahmadi, Baghban, Salwana et al. (2019)]:

$$\frac{min}{\omega,b,e} J(\omega,e) = \frac{1}{2}\omega^T\omega + \frac{1}{2}\gamma \sum_{k=1}^{N} e_k^2 \tag{2}$$

Which is related to the below constraints:

$$y_k = \omega^T\varphi(x_k) + b + e_k \qquad \text{k=1,2,...,N} \tag{3}$$

The Lagrangian equation is constructed to solve the optimization problem:

$$L(\omega,\text{b},\text{e},\alpha) = J(\omega,e) - \sum_{k=1}^{N} \alpha_k \{\omega^T\varphi(x_k) + b + e_k - y_k\} \tag{4}$$

where Υ and e_k are known as regularization parameter and regression error. The α_k represents the support value. To solve the above problem, the above equation is differentiated with respect to the different parameters:

$$\frac{\partial L(\omega,\text{b},\text{e},\alpha)}{\partial \omega} = 0 \rightarrow \omega = \sum_{k=1}^{N} \alpha_k \, \varphi(x_k) \tag{5}$$

$$\frac{\partial L(\omega,\text{b},\text{e},\alpha)}{\partial b} = 0 \rightarrow \sum_{k=1}^{N} \alpha_k = 0 \tag{6}$$

$$\frac{\partial L(\omega,\text{b},\text{e},\alpha)}{\partial e_k} = 0 \rightarrow \alpha_k = \gamma e_k, \quad \text{k=1,2,...,N} \tag{7}$$

$$\frac{\partial L(\omega,\text{b},\text{e},\alpha)}{\partial \alpha_k} = 0 \rightarrow y_k = \omega^T\varphi(x_k) + b + e_k \qquad \text{k=1,2,...,N} \tag{8}$$

Karush-Kuhn-Trucker matrix can be obtained by elimination of ω and e [Cortes and Vapnik (1995); Baylar, Hanbay and Batan (2009); Mehdizadeh and Movagharnejad (2011)]:

$$\begin{bmatrix} 0 & 1_v^T \\ 1_v & \Omega + \gamma^{-1}I \end{bmatrix} \begin{bmatrix} b \\ \alpha \end{bmatrix} = \begin{bmatrix} 0 \\ y \end{bmatrix} \tag{9}$$

where $y = [y_1 \ldots y_N]^T$, $\alpha = [\alpha_1 \ldots \alpha_N]^T$, $1_N = [1 \ldots 1]^T$, and I represent the identity matrix. $\mathbf{\Omega}_{kl}$ is $\varphi(x_k)^T \varphi(x_l) = K(x_k, x_l)$. $K(x_k, x_l)$ is known as kernel function which can be in different forms of linear, polynomial and radial basis function forms [Gunn (1998)]. The estimating function form of LSSVM algorithm can be expressed as following formulation [Muller, Mika, Ratsch et al. (2001); Rostami, Baghban and Shirazian (2019)]:

$$y(x) = \sum_{k=1}^{N} \alpha_k K(x, x_k) + b \tag{10}$$

2.4 Adaptive neuro-fuzzy inference system (ANFIS)

In Adaptive neuro-fuzzy inference system, which is called the ANFIS algorithm, in brief, has five different layers. The aforementioned approach was developed by Jang et al. [Jang, Sun and Mizutani (1997)]. The hybrid learning approach and backpropagation are known as fundamentals of training of conventional ANFIS algorithm [Qasem, Samadianfard and Nahand (2019); Rezakazemi, Mosavi and Shirazian (2019)]. The ANFIS algorithm was born base on fuzzy logic and neural network advantages and also the different evolutionary methods such as Imperialist Competitive Algorithm (ICA), Particle Swarm Optimization (PSO) and Genetic algorithm (GA) can be used to reach the optimal structure of ANFIS algorithm [Afshar, Gholami and Asoodeh (2014), Khosravi, Nunes, Asad et al. (2018); Razavi, Sabaghmoghadam, Bemani et al. (2019)]. The ANFIS structure is demonstrated in Fig. 1. As shown, there are two input variables and one output.
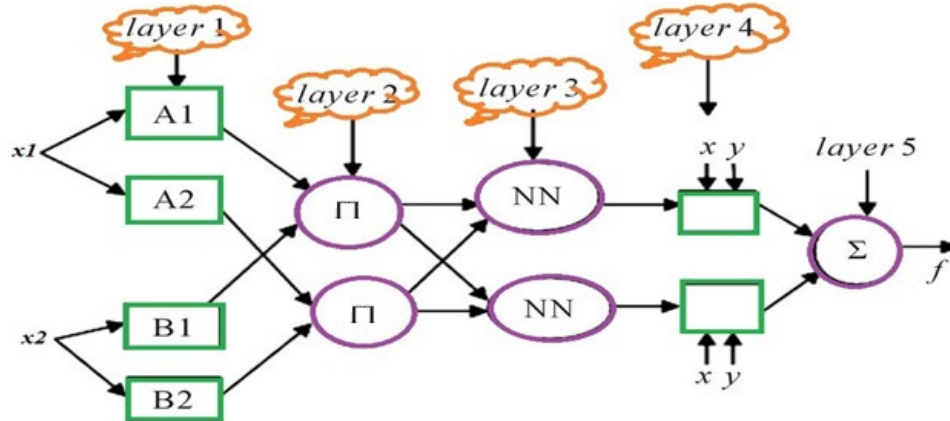

Figure 1: Typical construction of ANFIS approach

In the first layer, the linguistic terms are built based on input data. The Gaussian membership function is applied to organize these linguistic terms. The Gaussian function can be shown as the following formulation [Ahangari, Moeinossadat and Behnia (2015); Bahadori, Baghban, Bahadori et al. (2016)]:

$$O_i^1 = \beta(X) = exp^{(-\frac{1}{2}\frac{(X-Z)^2}{\sigma^2})} \tag{11}$$

where Z and σ denote the Gaussian parameters.

The next layer, shown as Π multiplies the incoming signals and contains the weighted terms which are related to rules:

$$O_i^2 = W_i = \beta_{Ai}(X) . \beta_{Bi}(X) \tag{12}$$

The third layer the shown as NN, it averages of determined weights are evaluated such as the following formulation:

$$O_i^3 = \frac{W_i}{\sum W_i} \tag{13}$$

Then in the next layer, the average weight values are multiplied to the related function such as below:

$$O_i^4 = \overline{W_i} f_i = \overline{W_i}(m_i X_1 + n_i X_2 + r_i) \tag{14}$$

where, m, n, and r represent the resulting indexes.

At last, the fifth layer consists of the summation of previous layer outputs:

$$O_i^5 = Y = \sum_i \overline{W_i} f_i = \overline{W_1} f_1 + \overline{W_2} f_2 = \frac{\sum W_i f_i}{\sum W_i} \tag{15}$$

2.5 Particle swarm optimization (PSO)

The combination of random probability distribution approach and generation of the population constructed the particle swarm optimization algorithm. Eberhart et al. introduced the PSO algorithm that comes from the social behavior of birds and developed it to solve nonlinear function optimization problems [Kennedy (2010)]. This strategy has special similarities with other optimization approaches such as a genetic algorithm that is constructed a base on a random solution population. Each particle can be known as a probable solution to the problem. A random population of particles created in search space to relate in an optimum system. P_{best} is known as the best solution which can be obtained from this strategy for a particle. Also, g_{best} represents the global best solution determined by the swarm. The particle moves in the space by time iterations, and the next iteration velocity is determined by using g_{best}, P_{best} and current velocity [Eberhart and Kennedy (1995)]. The P'th particle can be determined as follow:

$$X_{pd}^{iter+1} = X_{pd}^{iter} + V_{pd}^{iter+1} \tag{16}$$

The particle velocity is updated by the following expression:

$$v_{id}(t+1) = wv_{id}(t) + c_1 r_1 \left(p_{best,id}(t) - X_{iid}(t)\right) + c_2 r_2 \left(g_{best,d}(t) - X_{id}(t)\right) \tag{17}$$

w, c, and *r* are inertia weight, learning rate, and random number respectively [Haratipour, Baghban, Mohammadi et al. (2017)].

3 Results and discussion

In the present study, the determined structure of the MLP-ANN algorithm utilizes log-sigmoid, and linear activation functions the hidden and output layers respectively. By utilization of trial and error, the optimum number of neurons in hidden layers is determined as 7 to reach the best structure of the MLP-ANN algorithm. The performance of Levenberg Marquardt training of MLP-ANN algorithm based on the mean square error is shown in Fig. 2.
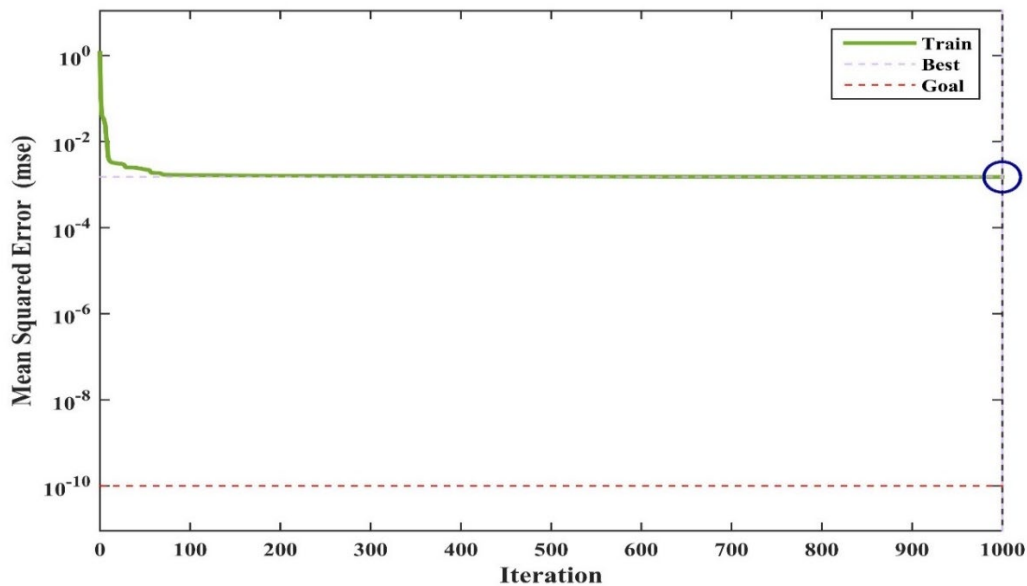
Figure 2: Trained MLP-ANN model by Levenberg Marquardt algorithm

In the RBF-ANN algorithm, the radial basis function (RBF) is utilized for hidden layers. According to information in the literature, the hidden layer neurons for RBF-ANN can be supposed one-tenth of training data points. The training process of the RBF-ANN algorithm base on MSE has been reported in Fig. 3.
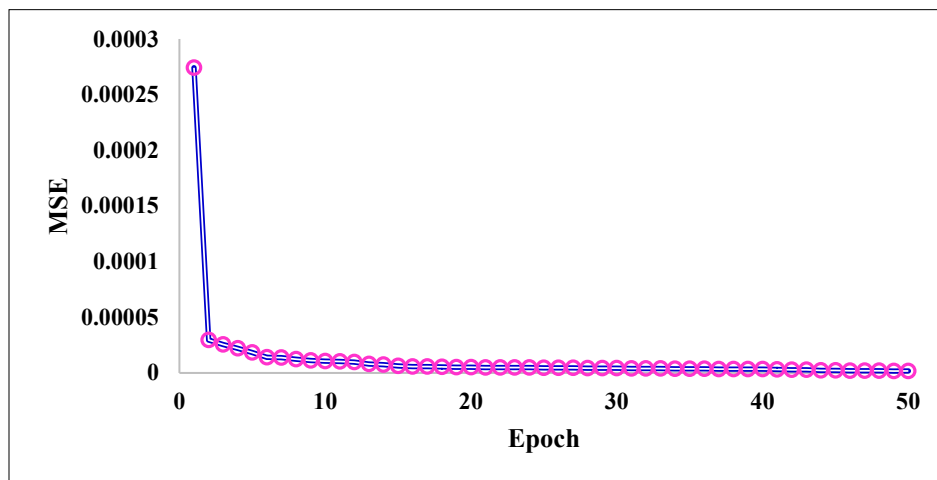

Figure 3: Trained RBF-ANN approach by Levenberg Marquardt algorithm

In this work, a particle swarm optimization approach is applied to train the best structure of the ANFIS algorithm. Fig. 4 demonstrates the gained root mean squared error (RMSE) of estimated and experimental acid solubility values in the training step.
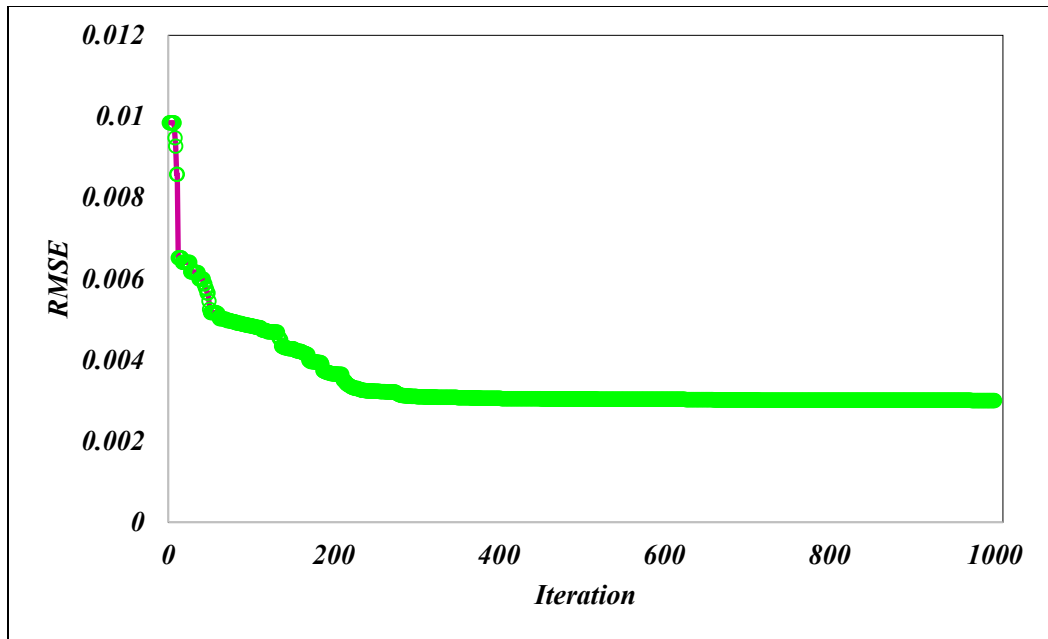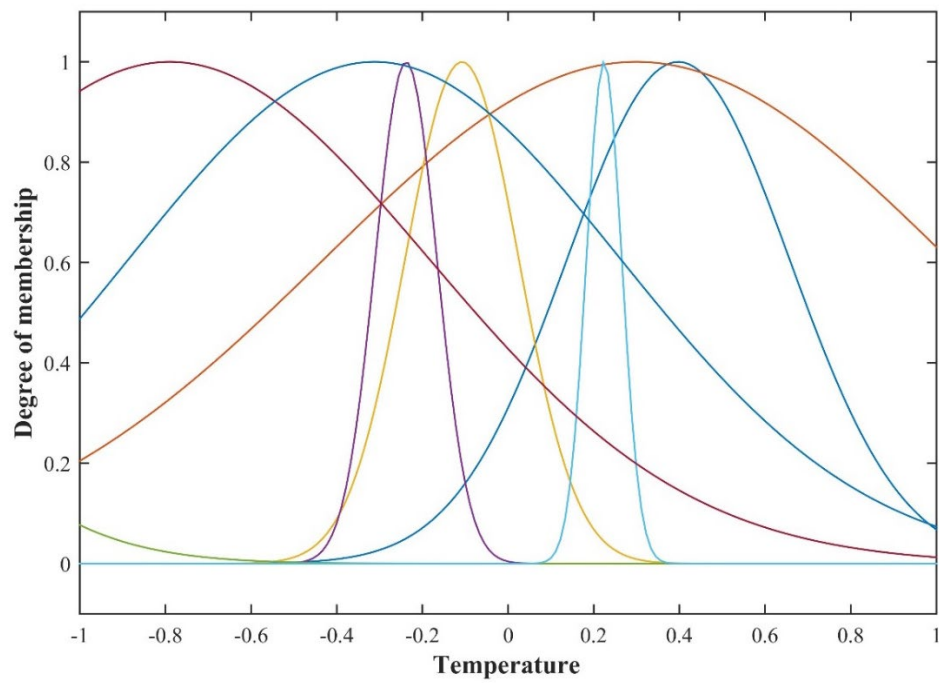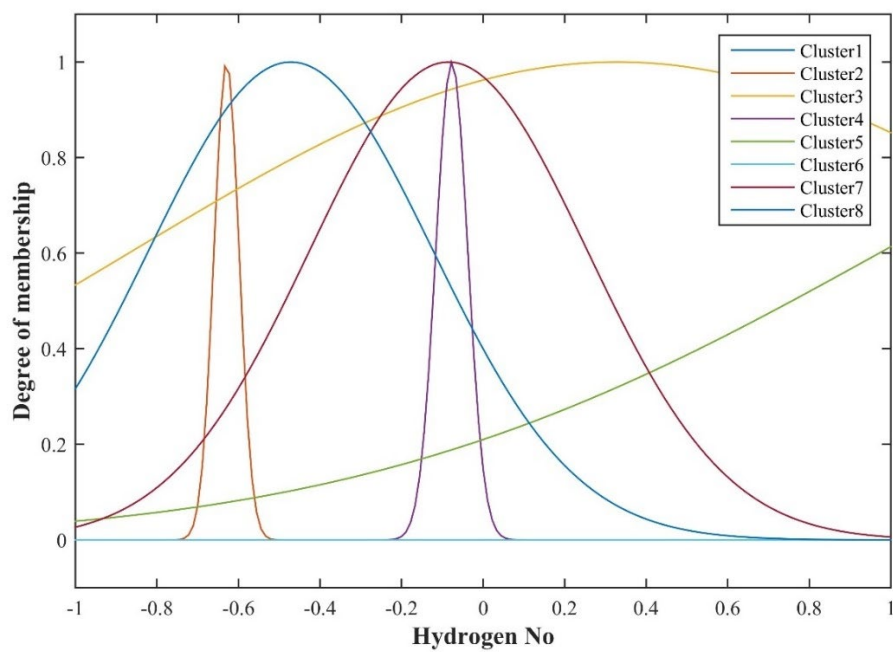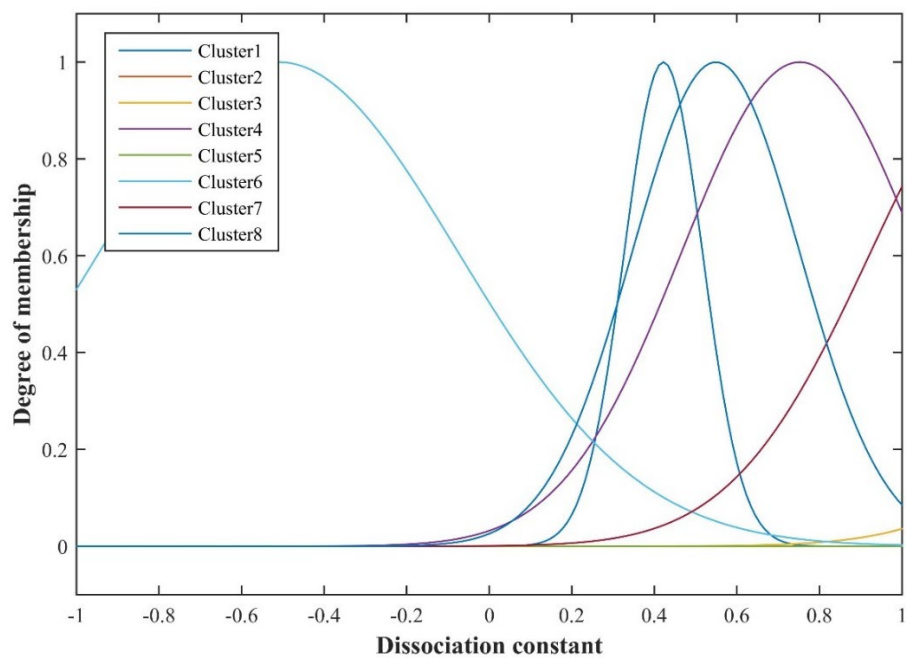
Figure 4: Performance of trained ANFIS model

The optimum structure of ANFIS can be recognized by the RMSE value of 0.003 after 1000 of iteration steps. Trained membership functions of the proposed ANFIS model are also shown in Fig. 5 for each cluster.
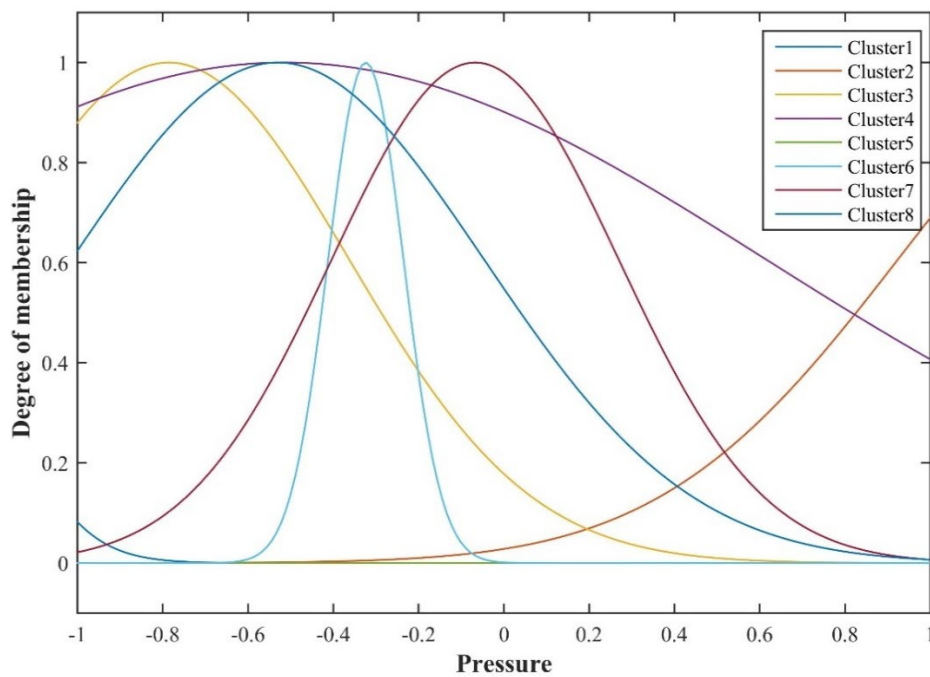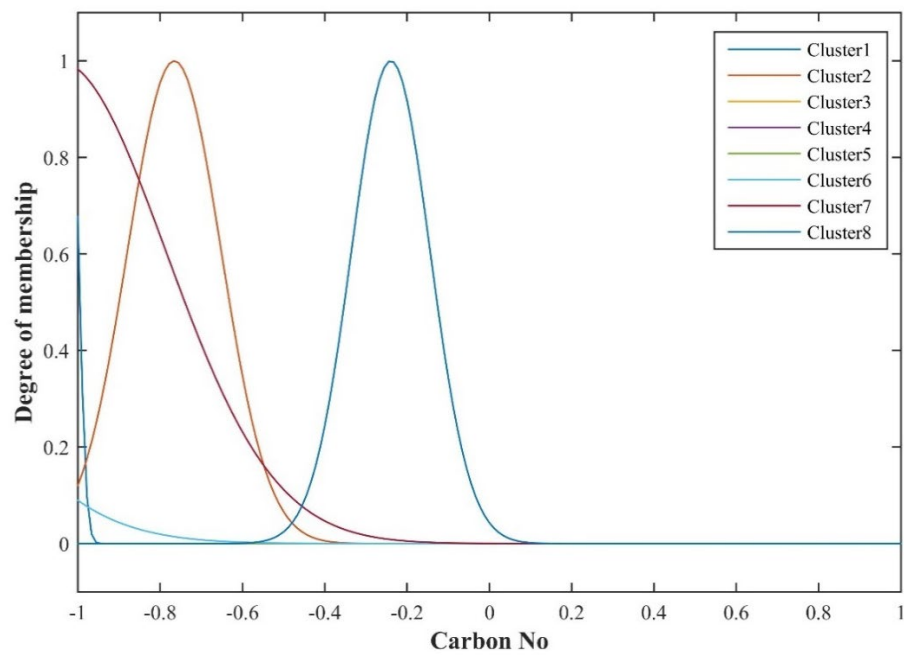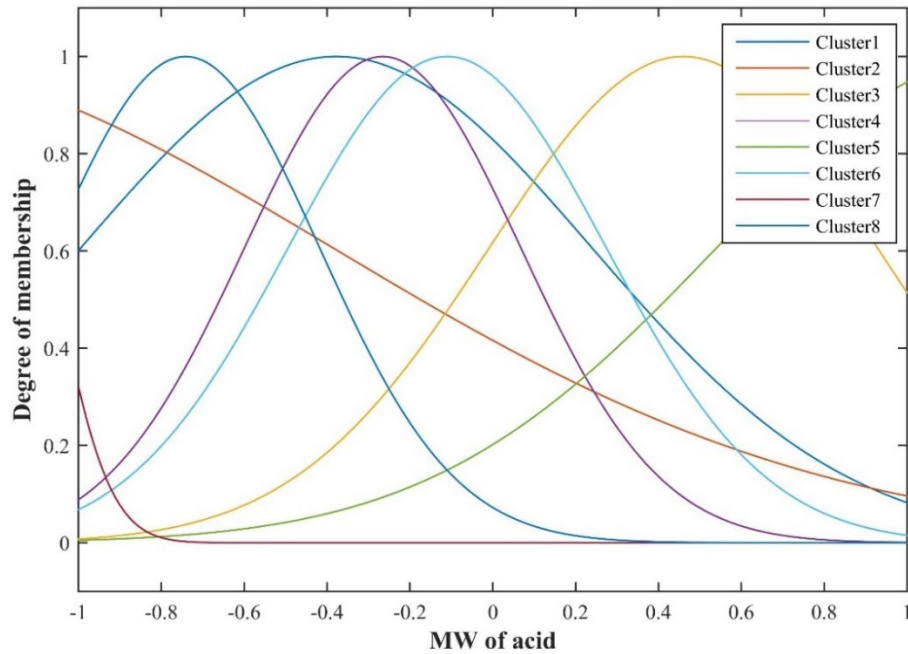
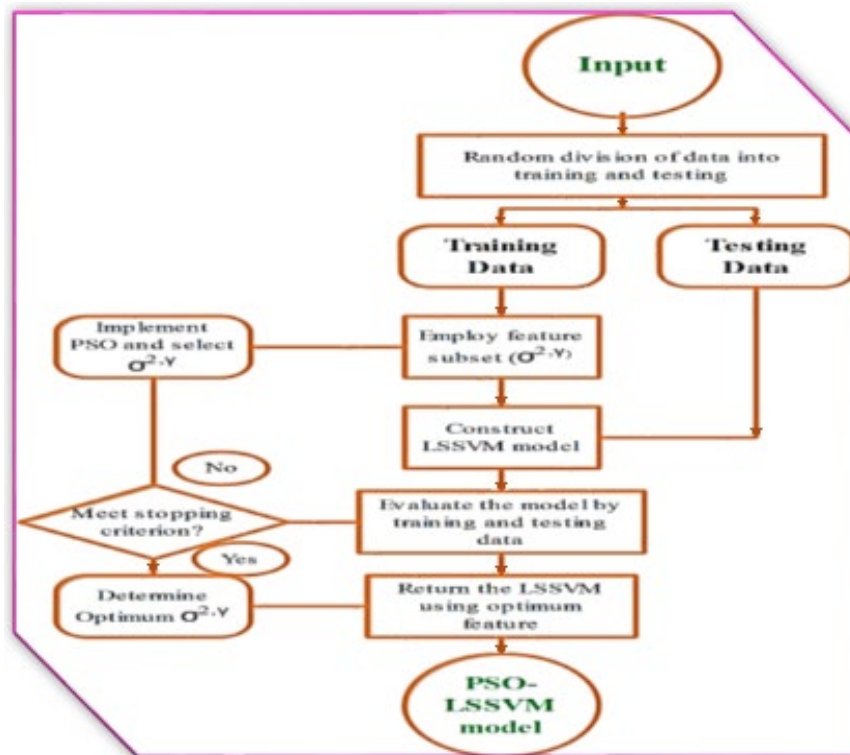**Figure 5:** Trained membership function parameters

Figure 6: Schematic demonstration of trained LSSVM algorithm

The RBF kernel function due to its high degree of performance is utilized to construct the LSSVM algorithm. The LSSVM algorithm has two tuning parameters, σ^2, and Υ which are determined by utilizing the PSO algorithm. The schematic demonstration of the LSSVM algorithm is depicted in Fig. 6. The details of predicting models are summarized in Tab. 1. These details can be helpful in the development of models for the prediction of acid solubility in carbon dioxide.

Table 1: Details of proposed models

Type	comment/value	Type	comment/value
LSSVM		ANFIS	
Kernel function	RBF	Membership function	Gaussian
σ^2	0.80321	No. of membership function parameters	112
Υ	12893.2264	No. of clusters	8
Number of data utilized for training	141	Number of data utilized for training	141
Number of data utilized for testing	47	Number of data utilized for testing	47
Population size	85	Population size	50
Iteration	1000	Iteration	1000
C1	1	C1	1
C2	2	C2	2
MLP-ANN		RBF-ANN	
No. input neuron layer	6	No. input neuron layer	6
No. hidden neuron layer	8	No. hidden neuron layer	50
No. output neuron layer	1	No. output neuron layer	1
Hidden layer activation function	Sigmoid	Hidden layer activation function	RBF
output layer activation function	Linear	output layer activation function	linear
Number of data utilized for training	141	Number of data utilized for training	141
Number of data utilized for testing	47	Number of data utilized for testing	47
Number of max iteration	1500	Number of max iteration	50

In order to show the performance of proposed models in the prediction of solubility of different acids, regression plots of RBF-ANN, MLP-ANN, ANFIS, and LSSVM algorithms are depicted in Fig. 7 to compare the determined and actual solubility values. Based on these plots, the surprising fits for the predicting algorithms are obtained. Also, the predicted acid solubility data for proposed models are demonstrated along with the corresponding actual acid solubility values in Fig. S1. It can be observed that the model's output solubility values have excellent agreement with actual solubility values. Another graphical evaluation method is a demonstration of relative error between predicted and experimental acid solubility in supercritical carbon dioxide. Fig. S2 shows the percentage of absolute error for the different predicting algorithms. The percentages of absolute error place under 1.5 percent for all developed algorithms, which expresses the acceptable degree of accuracy in prediction of acid solubility.
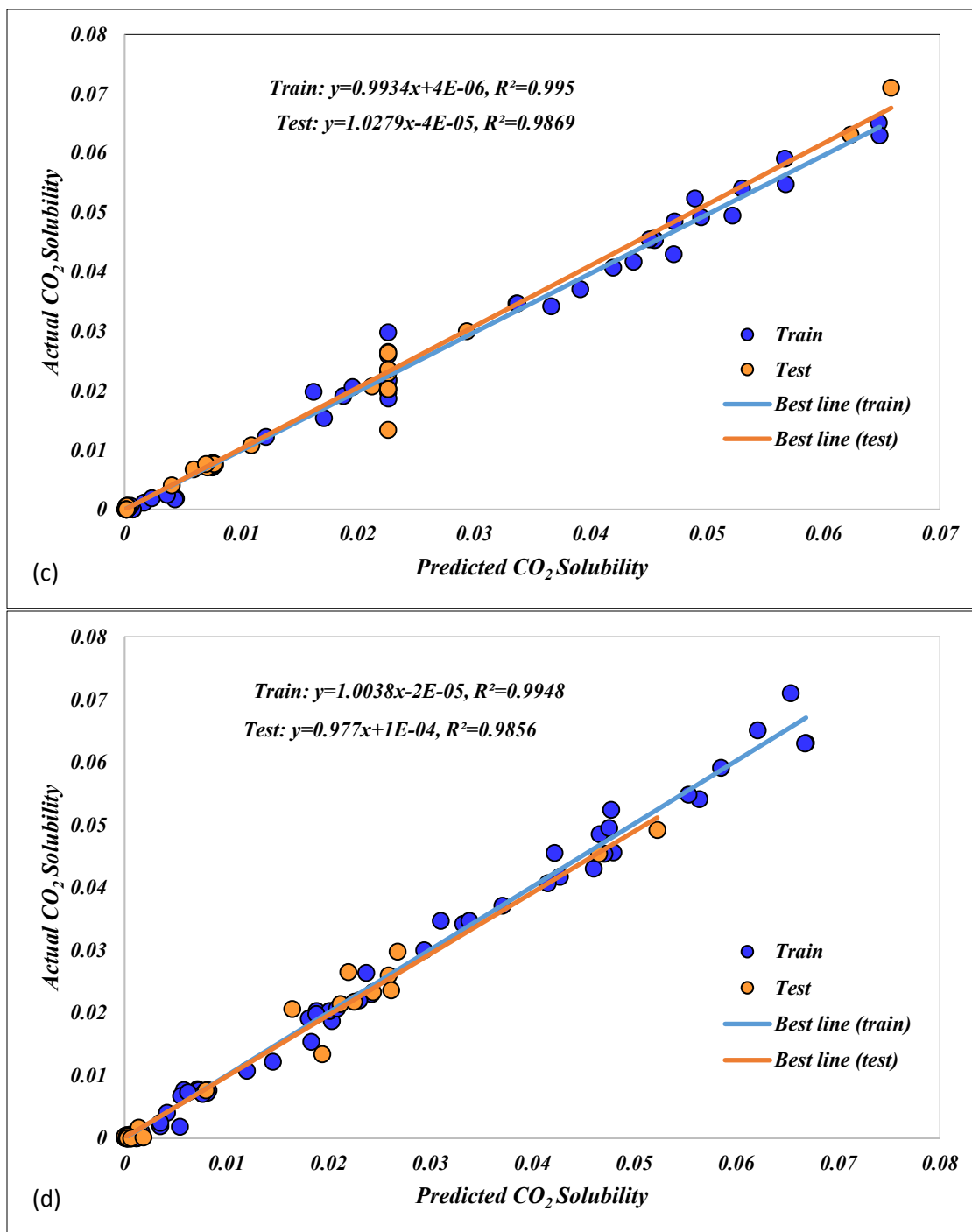
(a)

(b)
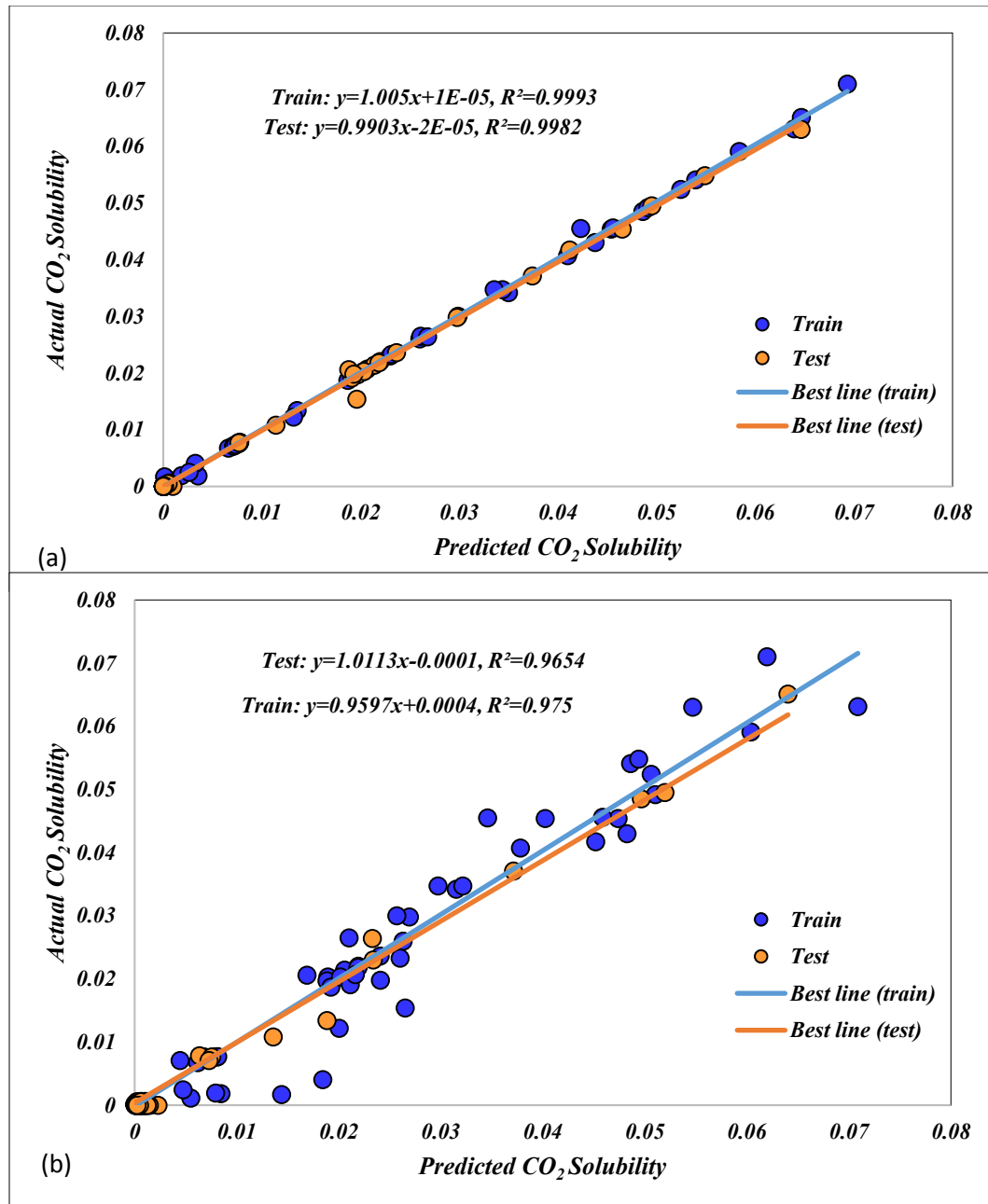
Figure 7: Regression plots obtained for different models

Furthermore, in order to clarify the performance of predicting algorithms, the statistical analysis is required so the coefficients of determination (R^2), average absolute deviation

(AAD), Mean squared errors (MSEs) and Standard deviations (STDs) are determined such as following:

$$R^2 = 1 - \frac{\sum_{i=1}^{N}(X_i^{actual} - X_i^{predicted})^2}{\sum_{i=1}^{N}(X_i^{actual} - \overline{X^{actual}})^2} \tag{18}$$

$$AAD = \frac{1}{N}\sum_{i=1}^{N}\left|X_i^{predicted} - X_i^{actual}\right| \tag{19}$$

$$MSE = \frac{1}{N}\sum_{i=1}^{N}(X_i^{actual} - X_i^{predicted})^2 \tag{20}$$

$$STD_{error} = \left(\frac{1}{N-1}\sum_{i=1}^{N}(error - \overline{error})\right)^{0.5} \tag{21}$$

The R^2, AD, MSE and STD values of different algorithms are summarized in Tab. 2. According to these results, the LSSVM model has the greatest ability in forecasting acid solubility. The determined R^2 values for LSSVM is equal to 0.998 and 0.999 in the train and test set, respectively. Furthermore, it's RMSE, MSE and AAD parameters are 0.000527, 2.77875E-07, and 0.0179, respectively. According to these analyses LSSVM algorithm is known as the best predictor for the prediction of solubility of different acids.

Table 2: Statistical analyses of models

Model	Set	MSE	RMSE	R^2	STD	AAD (%)
LSSVM	Train	5.72159E-07	0.000756	0.998	0.0007	0.0269
	Test	1.7978E-07	0.000424	0.999	0.0004	0.0149
	Total	2.77875E-07	0.000527	0.999	0.0005	0.0179
ANFIS	Train	5.79633E-06	0.002408	0.975	0.0022	0.1093
	Test	1.00976E-05	0.003178	0.965	0.0027	0.1677
	Total	9.02227E-06	0.003004	0.967	0.0026	0.1531
MLP-ANN	Train	3.23782E-06	0.001799	0.987	0.0017	0.0756
	Test	1.44839E-06	0.001203	0.995	0.0010	0.0600
	Total	1.89575E-06	0.001377	0.993	0.0012	0.0639
RBF-ANN	Train	2.33037E-06	0.001527	0.986	0.0013	0.0827
	Test	1.61993E-06	0.001273	0.995	0.0010	0.0779
	Total	1.79754E-06	0.001341	0.993	0.0011	0.0791

In addition to previous statistical indexes, there is another statistical approach to evaluate the reliability and accuracy of predicting algorithms, which called the Leverage method. The mentioned approach consists of some statistical concepts such as model residuals, Hat matrix, and Williams plot which are used for the detection of suspected and outlier data. There is more description of the Leverage method in the literature [Rousseeuw and Leroy (2005)]. In this method, the residuals are estimated and inputs are utilized to build a matrix

called Hat matrix such as follow:

$$H = X(X^T X)^{-1} X^T \tag{22}$$

where X is the $m \times n$ matrix, which n and m are the numbers of model parameters and samples, respectively.

Fig. 8 illustrates the William plot for the proposed models. As shown in this figure, most of the data points are in the range of leverage limit of residuals for -3 to 3. The leverage limit is formulated, such as the following:

$$H^* = 3(n + 1)/m \tag{23}$$
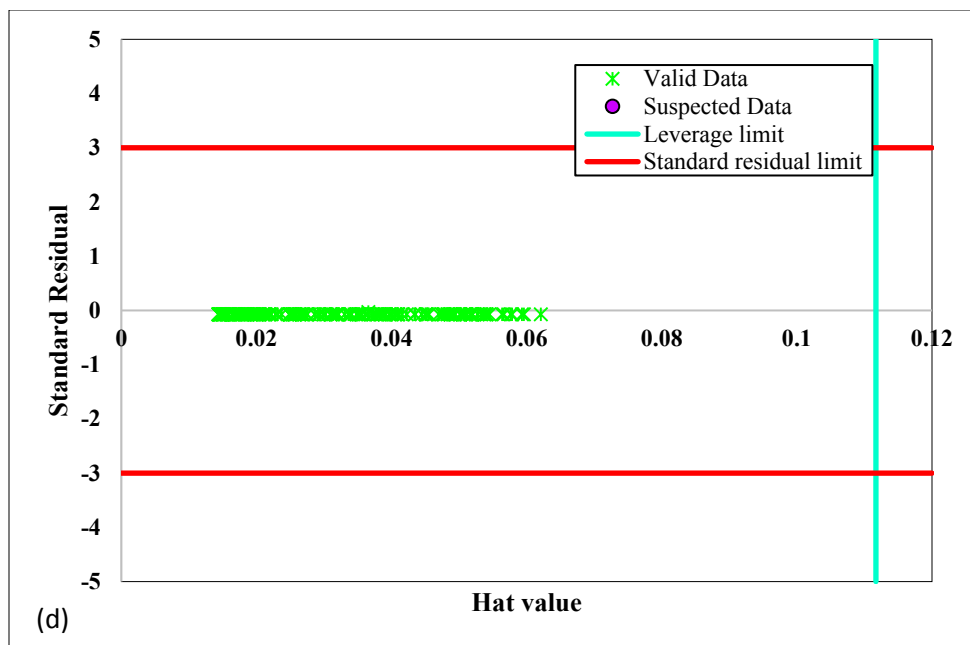

(a)

(b)

(c)
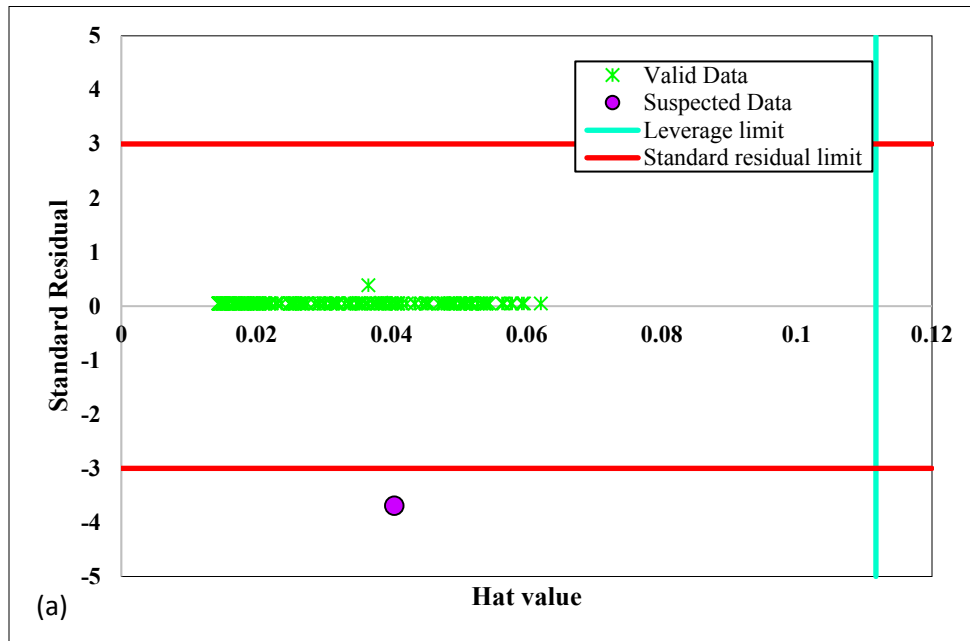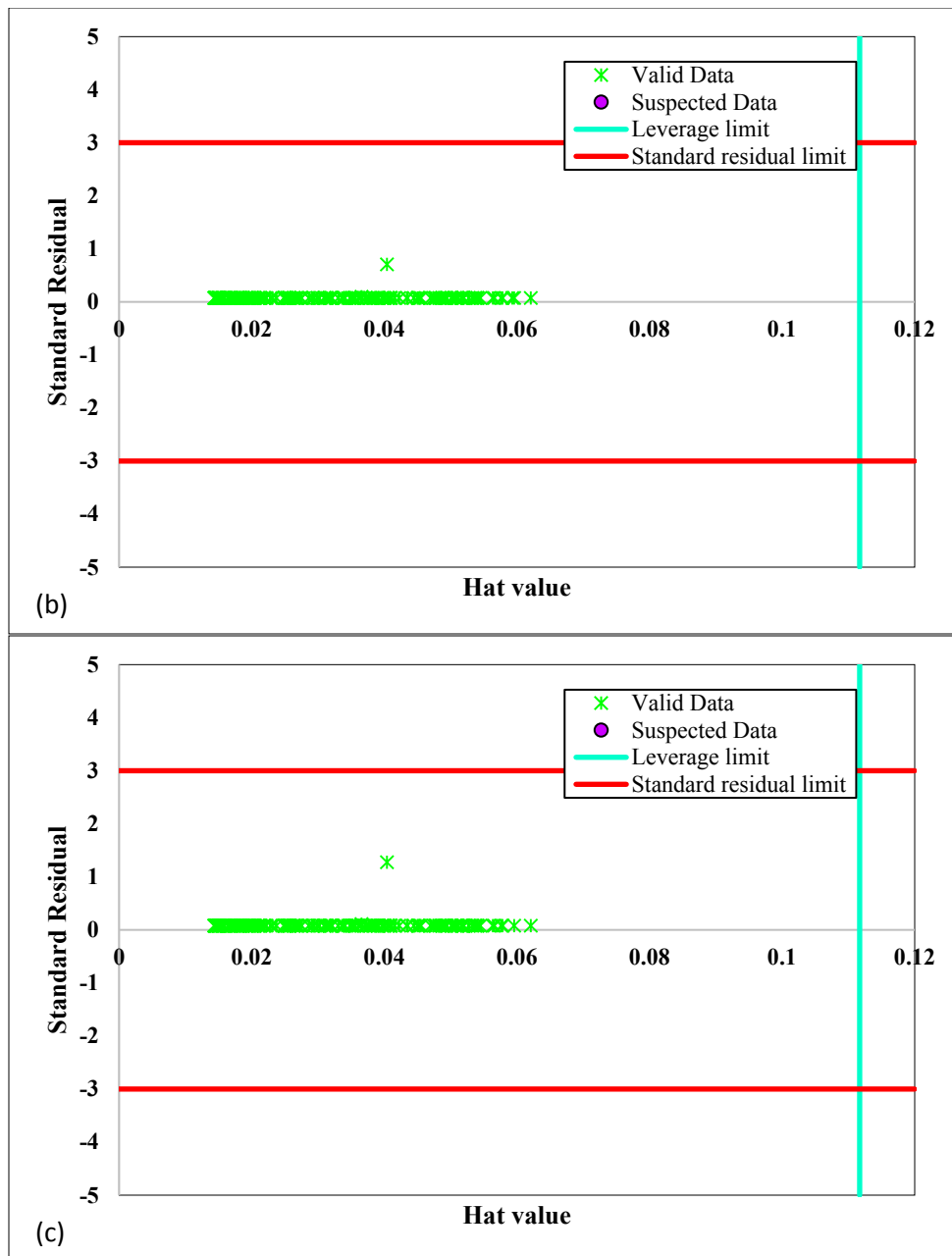
Figure 8: Absolute deviation plots for (a) LSSVM, (b) ANFIS, (c) MLP-ANN, and (d) RBF-ANN

Another method to investigate the validity of the models is a parametric analysis of solubility. To this end, the Relevancy index is introduced to investigate the impact of inputs on acid solubility. The Relevancy index is determined such as following [Zarei, Razavi, Baghban et al. (2019)]:

$$r = \frac{\sum_{i=1}^{n}(X_{k,i}-\overline{X_k})(Y_i-\overline{Y})}{\sqrt{\sum_{i=1}^{n}(X_{k,i}-\overline{X_k})^2 \sum_{i=1}^{n}(Y_i-\overline{Y})^2}} \tag{24}$$

where Y_i, $\overline{Y}$, $X_{k,i}$ and $\overline{X_k}$ are the 'i' th output, output average, kth of input and average of input. The Relevancy index absolute value represents the effectiveness of the parameters on acid solubility. As shown in Fig. 9, the molecular weight of acid has the most Relevancy factor between different input parameters, so this parameter is known as the most effective parameter on acid solubility in supercritical carbon dioxide. Moreover, acid dissociation constant has the least effect on acid solubility. This figure illustrates that as the number of carbon and hydrogen of acid, molecular weight, and pressure increases, acid solubility in carbon dioxide increases. On the other hand, increasing acid dissociation constant and temperature caused a drop in the solubility of acid in carbon dioxide.
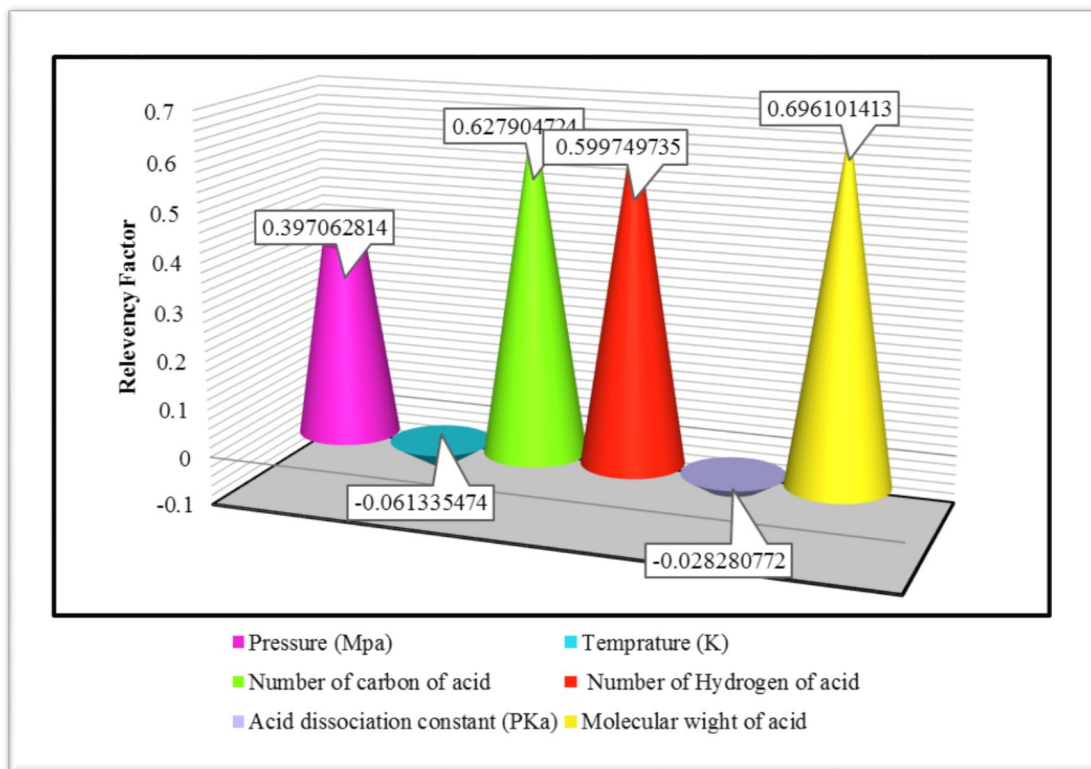
Figure 9: Sensitivity analysis of investigated variables

5 Conclusions

In this paper, we have applied RBF-ANN, MLP-ANN, ANFIS-PSO and LSSVM algorithms to determine the different acids solubility values in supercritical carbon dioxide in terms of pressure, temperature, and different acid structure based on a reliable databank which gathered from the literature. These predicting approaches can forecast acid solubility in a wide range of operating conditions. To prove the acclaim above, different statistical and graphical evaluations have been performed in the previous section. According to the obtained results from comparisons, the LSSVM model has the best performance respect to the others, and the ANFIS algorithm has the least accuracy in this prediction. Also, the results of the sensitivity analysis identify the molecular weight of the acid parameter is the most effective factor in the solubility of acids in supercritical carbon dioxide. Based on these comprehensive investigations, this manuscript has great potential and ability to help the researchers in their future works.

Conflicts of Interest: The authors declare that they have no conflicts of interest to report regarding the present study.

References

Abdi-Khanghah, M.; Bemani, A.; Naserzadeh, Z. (2018): Prediction of solubility of N-alkanes in supercritical CO_2 using RBF-ANN and MLP-ANN. *Journal of CO_2 Utilization,* vol. 25, pp. 108-119.

Afshar, M.; Gholami, A.; Asoodeh, M. (2014): Genetic optimization of neural network and fuzzy logic for oil bubble point pressure modeling. *Korean Journal of Chemical Engineering*, vol. 31, no. 3, pp. 496-502.

Ahangari, K.; Moeinossadat, S. R.; Behnia, D. (2015): Estimation of tunnelling-induced settlement by modern intelligent methods. *Soils and Foundations*, vol. 55, no. 4, pp. 737-748.

Ahmadi, M. H.; Baghban, A.; Salwana, E.; Sadeghzadeh, M.; Zamen, M. et al. (2019): Machine learning prediction models of electrical efficiency of photovoltaic-thermal collectors. *Energies*, vol. 8, pp. 120-144.

Baghban, A.; Bahadori, M.; Lemraski, A. S.; Bahadori, A. (2016): Prediction of solubility of ammonia in liquid electrolytes using least square support vector machines. *Ain Shams Engineering Journal*, vol. 12, pp. 99-120.

Baghban, A.; Namvarrechi, S.; Phung, T. K.; Lee, M. (2016): Phase equilibrium modelling of natural gas hydrate formation conditions using LSSVM approach. *Petroleum Science and Technology*, vol. 34, no. 16, pp. 1431-1438.

Bahadori, A.; Baghban, A.; Bahadori, M.; Lee, M.; Ahmad, Z. (2016): Computational intelligent strategies to predict energy conservation benefits in excess air controlled gas-fired systems. *Applied Thermal Engineering*, vol. 102, pp. 432-446.

Bas, D.; Boyaci, I. H. (2007): Modeling and optimization I: usability of response surface methodology. *Journal of Food Engineering*, vol. 78, no. 3, pp. 836-845.

Baylar, A.; Hanbay, D.; Batan, M. (2009): Application of least square support vector machines in the prediction of aeration performance of plunging overfall jets from weirs. *Expert Systems with Applications*, vol. 36, no. 4, pp. 8368-8374.

Belghait, A.; Si-Moussa, C.; Laidi, M.; Hanini, S. (2018): Semi-empirical correlation of solid solute solubility in supercritical carbon dioxide: comparative study and proposition of a novel density-based model. *Comptes Rendus Chimie*, vol. 7, pp. 87-99.

Bovard, S.; Abdi, M.; Nikou, K.; Daryasafar, A. (2017): Numerical investigation of heat transfer in supercritical CO_2 and water turbulent flow in circular tubes. *Journal of Supercritical Fluids*, vol. 119, pp. 88-103.

Celso, F. L.; Triolo, A.; McClain, J. (2002): Industrial applications of the aggregation of block copolymers in supercritical CO_2: a SANS study. *Applied Physics A*, vol. 74, no. 1, pp. 1427-1429.

Choubin, B.; Abdolshahnejad, M.; Moradi, E. (2020): Spatial hazard assessment of the PM10 using machine learning models in Barcelona, Spain. *Science of The Total Environment*, vol. 701, pp. 166-182.

Cortes, C.; Vapnik, V. (1995): Support-vector networks. Machine learning. vol. 20, no.

3, pp. 273-297.

Dartiguelongue, A.; Leybros, A.; Grandjean A. (2016): Solubility of perfluoropentanoic acid in supercritical carbon dioxide: measurements and modeling. *Journal of Chemical & Engineering Data*, vol. 61, no. 11, pp. 3902-3907.

Eberhart, R.; Kennedy, J. (1995): A new optimizer using particle swarm theory. *Micro Machine and Human Science, Energy IEEE*, vol. 33, pp. 345-366.

Erkey, C. (2000): Supercritical carbon dioxide extraction of metals from aqueous solutions: a review. *Journal of Supercritical Fluids*, vol. 17, no. 3, pp. 259-287.

Faizollahzadeh, A.; Najafi, B.; Alizamir, M.; Mosavi, A. (2018): Using SVM-RSM and ELM-RSM approaches for optimizing the production process of methyl and ethyl esters. *Energies*, vol. 11, no. 11, 2889.

Fei, C.; Olsen, J. (2011): Prenatal exposure to perfluorinated chemicals and behavioral or coordination problems at age 7 years. *Environmental Health Perspectives*, vol. 119, no. 4, pp. 573-390.

Gao, W.; Daryasafar, A.; Lavasani, M. (2018): Flow reversal of laminar mixed convection for supercritical CO_2 flowing vertically upward in the entry region of asymmetrically heated annular channel. *Journal of Supercritical Fluids,* vol. 131, pp. 87-98.

Ghaziaskar, H. S.; Afsari, S.; Rezayat, M.; Rastegari, H. (2017): Quaternary solubility of acetic acid, diacetin and triacetin in supercritical carbon dioxide. *Journal of Supercritical Fluids*, vol. 119, pp. 52-57.

Ghaziaskar, H. S.; Kaboudvand, M. (2008): Solubility of trioctylamine in supercritical carbon dioxide. *Journal of Supercritical Fluids*, vol. 44, no. 2, pp. 148-154.

Ghaziaskar, H. S.; Nikravesh, M. (2003): Solubility of hexanoic acid and butyl acetate in supercritical carbon dioxide. *Fluid Phase Equilibria*, vol. 206, no. 1, pp. 215-221.

Gunn, S. R. (1998): Support vector machines for classification and regression. *ISIS Technical Report*, vol. 14, no. 1, pp. 5-16.

Gurdial, G. S.; Foster, N. R. (1991): Solubility of o-hydroxybenzoic acid in supercritical carbon dioxide. *Industrial & Engineering Chemistry Research*, vol. 30, no. 3, pp. 575-580.

Haratipour, P.; Baghban, A.; Mohammadi, A. H.; Nazhad, S.; Bahadori, A. (2017): On the estimation of viscosities and densities of CO_2-loaded MDEA, MDEA+AMP, MDEA+DIPA, MDEA+MEA, and MDEA+DEA aqueous solutions. *Journal of Molecular Liquids*, vol. 242, pp. 146-159.

Hemmati-Sarapardeh, A.; Hajirezaie, S. (2020): Modeling natural gas compressibility factor using a hybrid group method of data handling. *Engineering Applications of Computational Fluid Mechanics*, vol. 14, no. 1, pp. 27-37.

Hintzer, K.; Juergens, M.; Kaempf, G. J.; Kaspar, H.; Lochhaas, K. H. (2016): *Fluoropolymer Compositions and Purification Methods Thereof*, USA.

Hintzer, K.; Löhr, G.; Killich A.; Schwertfeger, W. (2004): *Method of Making an Aqueous Dispersion of Fluoropolymers*, USA.

Huang, Z.; Chiew, Y. C.; Lu, W. Kawi, S. (2005): Solubility of aspirin in supercritical carbon dioxide/alcohol mixtures. *Fluid Phase Equilibria*, vol. 237, no. 1, pp. 9-15.

Hubbard, H.; Guo, Z.; Krebs, K.; Metzger, S. (2012): *Removal of Perfluorocarboxylic Acids (PFCAS) from Carpets Treated with Stain-Protection Products by Using Carpet Cleaning Machines.*

Inomata, H.; Honma, Y.; Imahori, M.; Arai, K. (1999): Fundamental study of de-solventing polymer solutions with supercritical CO_2. *Fluid Phase Equilibria*, vol. 158, pp. 857-867.

Jang, J. R.; Sun, C.; Mizutani, E. (1997): Neuro-fuzzy and soft computing: a computational approach to learning and machine intelligence. *Computers*, vol. 33, pp. 939-960.

Kennedy, J. (2010): Particle swarm optimization encyclopedia of machine learning, *Springer Computers*, vol. 7, pp. 760-766.

Khosravi, A.; Nunes, R.; Assad M.; Machado, L. (2018): Comparison of artificial intelligence methods in estimation of daily global solar radiation. *Journal of Cleaner Production*, vol. 194, pp. 342-358.

Knez, Z.; Cor, D. (2017): Solubility of solids in sub-and supercritical fluids: a review 2010-2017. *Journal of Chemical & Engineering Data*, vol. 33, no. 11, pp. 122-141.

Kumoro, A. C. (2011): Solubility of corosolic acid in supercritical carbon dioxide and its representation using density-based correlations. *Journal of Chemical & Engineering Data*, vol. 56, no. 5, pp. 2181-2186.

Lin, F.; Liu, D.; Maiti, S.; Das, N. (2014): Recent progress in heavy metal extraction by supercritical CO_2 fluids. *Industrial & Engineering Chemistry Research*, vol. 53, no. 5, pp. 1866-1877.

Mehdizadeh, B.; Movagharnejad, K. (2011): A comparative study between LS-SVM method and semi empirical equations for modeling the solubility of different solutes in supercritical carbon dioxide. *Chemical Engineering Research and Design*, vol. 89, no. 11, pp. 2420-2427.

Moody, C. A.; Field, J. A. (1999): Determination of perfluorocarboxylates in groundwater impacted by fire-fighting activity. *Environmental Science & Technology*, vol. 33, no. 16, pp. 2800-2806.

Mosavi, A., Shamshirband, S.; Salwana, E.; Chau, K. W.; Tah, J. H. (2019): Prediction of multi-inputs bubble column reactor using a novel hybrid model of computational fluid dynamics and machine learning. *Engineering Applications of Computational Fluid Mechanics*, vol. 13, no. 1, pp. 482-492.

Mosavi, A., Salimi, M., Faizollahzadeh, S. (2019): State of the art of machine learning models in energy systems, a systematic review. *Energies*, vol. 12, no. 7, pp. 1301.

Movagharnejad, K.; Mehdizadeh, B.; Banihashemi, M.; Kordkheili, M. S. (2011): Forecasting the differences between various commercial oil prices in the Persian Gulf region by neural network. *Energy*, vol. 36, no. 7, pp. 3979-3984.

Muller, R.; Mika, S.; Ratsch, G.; Tsuda, K.; Scholkopf, B. (2001): An introduction to kernel-based learning algorithms. *IEEE transactions on Neural Networks*, vol. 12, no. 2, pp. 181-201.

Munshi, P.; Bhaduri, S. (2009): Supercritical CO_2: a twenty-first century solvent for the chemical industry. *Current Science*, vol. 97, no. 1, pp. 442-460.

Najafi, B., Faizollahzadeh, S.; Mosavi, A.; Shamshirband, S.; Rabczuk, T. (2018): An intelligent artificial neural network-response surface methodology method for accessing the optimum biodiesel and diesel fuel blending conditions in a diesel engine from the viewpoint of exergy and energy analysis. *Energies*, vol. 11, no. 4, pp. 860.

Nahar, L.; Sarker, S. D. (2012): Supercritical fluid extraction in natural products analyses. *Natural Products Isolation, Springer*, vol. 9, pp. 43-74.

Ohde, H.; Hunt, F.; Wai, C. M. (2001): Synthesis of silver and copper nanoparticles in a water-in-supercritical-carbon dioxide microemulsion. *Chemistry of Materials*, vol. 13, no. 11, pp. 4130-4135.

Qasem, S. N.; Samadianfard, S.; Nahand, H. S. (2019): Estimating daily dew point temperature using machine learning algorithms. *Water*, vol. 11, no. 3, 582.

Razavi, R.; Sabaghmoghadam, A.; Bemani, A.; Baghban, A. (2019): Application of ANFIS and LSSVM strategies for estimating thermal conductivity enhancement of metal and metal oxide based nanofluids. *Engineering Applications of Computational Fluid Mechanics*, vol. 13, no. 1, pp. 560-578.

Rezakazemi, M.; Mosavi, A.; Shirazian, S. (2019): ANFIS pattern for molecular membranes separation optimization. *Journal of Molecular Liquids*, vol. 274, pp. 470-476.

Riahi-Madvar, H.; Dehghani, M. (2019): Comparative analysis of soft computing techniques RBF, MLP, and ANFIS with MLR and MNLR for predicting grade-control scour hole geometry. *Engineering Applications of Computational Fluid Mechanics*, vol. 13, no. 1, pp. 529-550.

Richter, H. P.; Dibble, E. J. (1983): *Repellent Coatings for Optical Surfaces*.

Rostami, A.; Baghban A.; Shirazian, S. (2019): On the evaluation of density of ionic liquids: towards a comparative study. *Chemical Engineering Research and Design*, vol. 76, pp. 323-345

Rousseeuw, P. J.; Leroy, **A. M.** (2005): *Robust Regression and Outlier Detection*. John Wiley & Sons.

Sahihi, M.; Ghaziaskar, H. S.; Hajebrahimi, M. (2010): Solubility of maleic acid in supercritical carbon dioxide. *Journal of Chemical & Engineering Data*, vol. 55, no. 7, pp. 2596-2599.

Shamshirband, S.; Hadipoor, M.; Baghban, A. (2019): Developing an ANFIS-PSO model to predict mercury emissions in combustion flue gases. *Mathematics*, vol. 7, no. 10, pp. 965-988.

Smith, M. (1993): *Neural Networks for Statistical Modeling*. Thomson Learning.

Sovova, H.; Zarevucka, M.; Vacek, M.; Stransky, K. (2001): Solubility of two vegetable oils in supercritical CO_2. *Journal of Supercritical Fluids*, vol. 20, no. 1, pp. 15-28.

Sparks, D. L.; Estevez, L. A.; Hernandez, R.; Barlow, K.; French, T. (2008): Solubility of nonanoic (pelargonic) acid in supercritical carbon dioxide. *Journal of Chemical & Engineering Data*, vol. 53, no. 2, pp. 407-410.

Sparks, D. L.; Hernandez, R.; Estévez, L. A.; Meyer, N.; French, T. (2007): Solubility of azelaic acid in supercritical carbon dioxide. *Journal of Chemical & Engineering Data*,

vol. 52, no. 4, pp. 1246-1249.

Stassi, A.; Bettini, R. (2000): Assessment of solubility of ketoprofen and vanillic acid in supercritical CO_2 under dynamic conditions. *Journal of Chemical & Engineering Data*, vol. 45, no. 2, pp. 161-165.

Sunarso, J.; Ismadji, S. (2009): Decontamination of hazardous substances from solid matrices and liquids using supercritical fluids extraction: a review. *Journal of Hazardous Materials*, vol. 161, no. 1, pp. 1-20.

Suykens, J. A.; Vandewalle, J. (1999): Least squares support vector machine classifiers. *Neural Processing Letters*, vol. 9, no. 3, pp. 293-300.

Suykens, J. A.; Vandewalle, J.; Moor, **B.** (2001): Optimal control by least squares support vector machines. *Neural Networks*, vol. 14, no. 1, pp. 23-35.

Tian, G.; Jin, J.; Guo, J.; Zhang, Z. (2007): Mixed solubilities of 5-sulfosalicylic acid and p-aminobenzoic acid in supercritical carbon dioxide. *Journal of Chemical & Engineering Data*, vol. 52, no. 5, pp. 1800-1802.

Uzer, S.; Akman U.; Hortacsu, C. (2006): Polymer swelling and impregnation using supercritical CO_2: a model-component study towards producing controlled-release drugs. *Journal of Supercritical Fluids*, vol. 38, no. 1, pp. 119-128.

Vapnik, V. (1998): *Statistical Learning Theory*. Wiley, New York.

Wang, Y. (2005): Characterization and expression of AmphiCL encoding cathepsin L proteinase from amphioxus Branchiostoma belcheri tsingtauense. *Marine Biotechnology*, vol. 7, no. 4, pp. 279-286.

Zamen, M. (2019): Optimization methods using artificial intelligence algorithms to estimate thermal efficiency of PV/T system. *Energy Science & Engineering*, vol. 8, pp. 87-97.

Zarei, F.; Razavi, R.; Baghban, A.; Mohammadi, H. (2019): Evolving generalized correlations based on Peng-Robinson equation of state for estimating dynamic viscosities of alkanes in supercritical region. *Journal of Molecular Liquids*, vol. 284, pp. 755-764.

Zhang, X.; Heinonen, S.; Levanen, E. (2014): Applications of supercritical carbon dioxide in materials processing and synthesis. *RSC Advances*, vol. 4. no. 105, pp. 61137-61152.

Zhao, Z.; Zhang, X.; Zhao, K.; Jiang, P.; Chen, Y. (2017): Numerical investigation on heat transfer and flow characteristics of supercritical nitrogen in a straight channel of printed circuit heat exchanger. *Applied Thermal Engineering*, vol. 126, pp. 717-729.

Appendix A. Nomenclature

ANFIS	**Adaptive neuro-fuzzy inference system**
LSSVM	Least squares support vector machine
RBF-ANN	Radial basis function artificial neural network
MLP-ANN	Multi-layer Perceptron artificial neural network
PSO	Particle swarm optimization

φ(x)	Nonlinear function
ω	Weight
b	Bias
ϒ	Regularization parameter
e_k	Support value
K	Kernel function
Z	Gaussian parameter
σ	Gaussian parameter
m	One of the resulting index of ANFIS
n	One of the resulting index of ANFIS
r	One of the resulting index of ANFIS
W	Inertia weight
c	Learning rate
R^2	Coefficient of determination
AAD	Average absolute deviation
MSE	Mean squared error
STD	Standard deviation
H	Hat matrix
H^*	The leverage limit

Appendix B. Supplementary Contents

Table S1: Experimental data which are used in this study
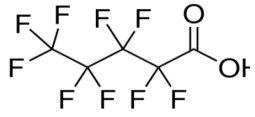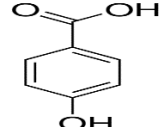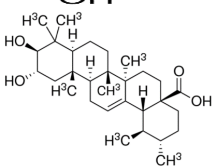
Acid name	Pressure	Temperature (K)	Acid dissociation constant (PKa)	solubility (mol/mol)	No of data points	Ref
Perfluoropentanoic acid	10-26.2	314-334	0.52	0.0134-0.0298	17	[Dartiguelongue, Leybros et al. 2016]
o-Hydroxybenzoic Acid	8.11-20.26	308.15-328.15	4.06	0.000007-0.000624	49	[Gurdial and Foster (1991)]
Corosolic Acid	8.0-30	308.15-333.15	4.7	3.28×10^{-11} - 0.071	40	[Kumoro (2011)]
Maleic Acid	7.0-30	318.15-348.15	1.83	0.000013-0.0005917	21	[Sahihi, Ghaziaskar, and Hajebrahimi (2010)]
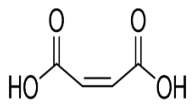
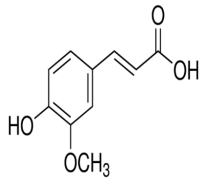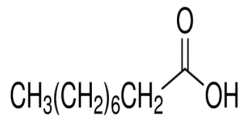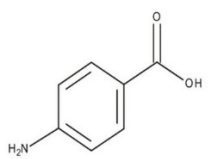|						
Ferulic Acid	12.0-28	301.15-333.15	4.38	0.00000155 -0.0000118	18	[Sovova, Zarevucka, Vacek et al. (2001)]
Azelaic Acid	10.0-30	313.15-333.15	4.84	0.00000042 - 0.00001012	14	[Sparks and Hernandez (2007)]
Nonanoic Acid	10.0-30	313.15-333.15	4.96	0.00013- 0.00782	14	[Sparks, Estévez, Hernandez et al. (2008)]
p-aminobanzoic acid	8.0-21	308-328.0	4.78	0.00000130 2- 0.00000645 2	15	[Tian, Jin, Guo et al. (2007)]
					Total=188	

Table S2: Average of experimental data which are used in this study

Acid name	Pressure (Mpa)	Temprature (K)	Solublity (mol/mol)
Perfluoropentanoic acid	17.37058824	324	0.022118
o-Hydroxybenzoic Acid	13.84040816	316.6193878	0.000238
Corosolic Acid	18.2	319.4	0.029932
Maleic Acid	16.42857143	333.15	0.000173
Ferulic Acid	19.83333333	319.4833333	5.37E-06
Azelaic Acid	20	323.15	3.92E-06
Nonanoic (Pelargonic) Acid	20	323.15	0.006548
p-aminobanzoic acid	14	318	3.82E-06

Table S3: Details of acids which are utilized in this investigation

Acid name	Structure	Empirical Formula or linear formula	Molecular Weight gr/mole
Perfluoropentanoic acid		$CF_3(CF_2)_3COOH$	264.05
o-Hydroxybenzoic Acid		$HOC_6H_4CO_2H$	138.12
Corosolic Acid		$C_{30}H_{48}O_4$	472.70

Maleic Acid		$HO_2CCH{=}CHCO_2H$	116.07
Ferulic Acid		$HOC_6H_3(OCH_3)CH{=}C$ HCO_2H	194.18
Azelaic Acid		$HO_2C(CH_2)_7CO_2H$	188.22
Nonanoic (Sparks, Estévez, Hernandez et al. 2008) Acid		$CH_3(CH_2)_7COOH$	158.24
p-aminobanzoic acid		$C_7H_7NO_2$	137.14
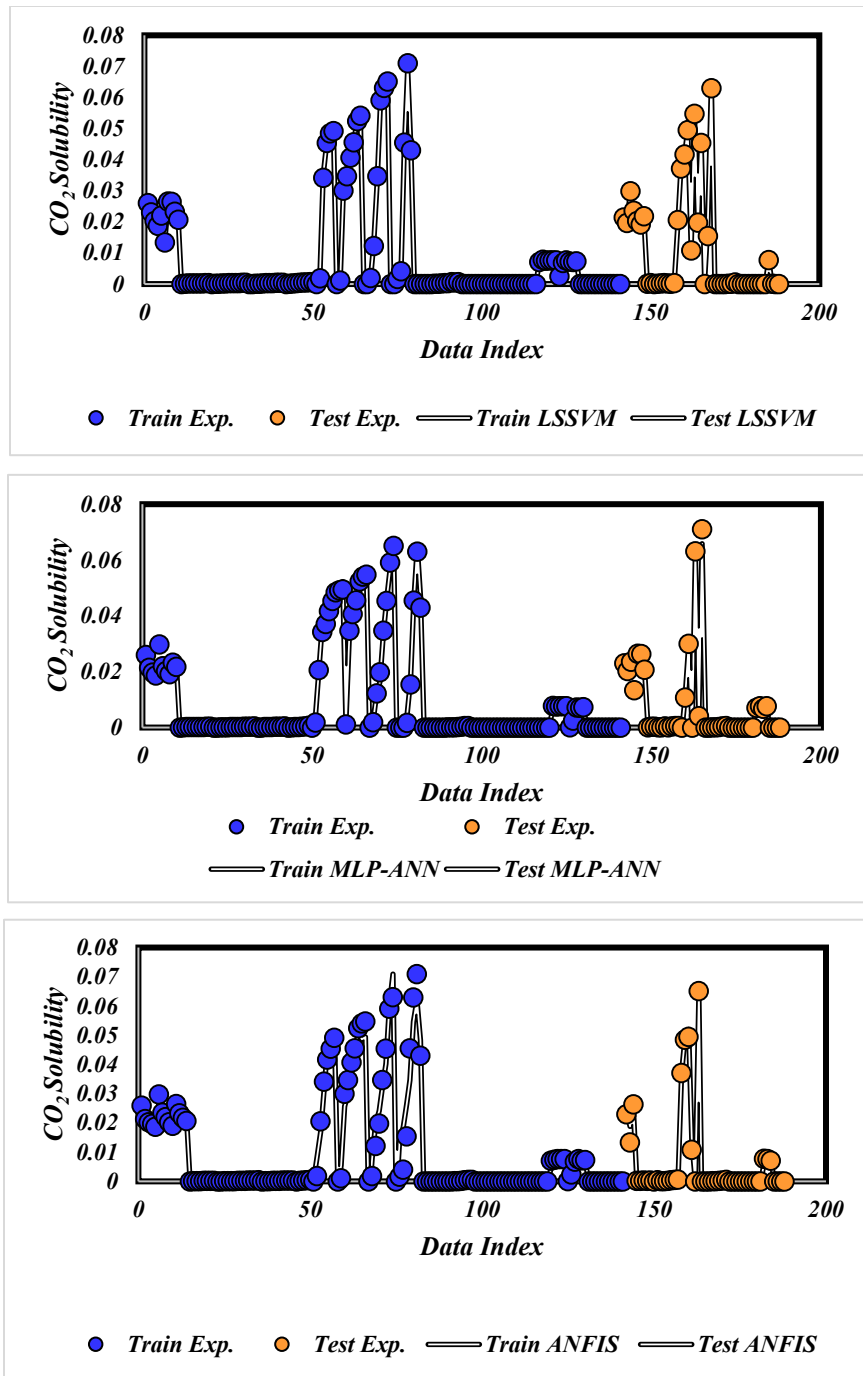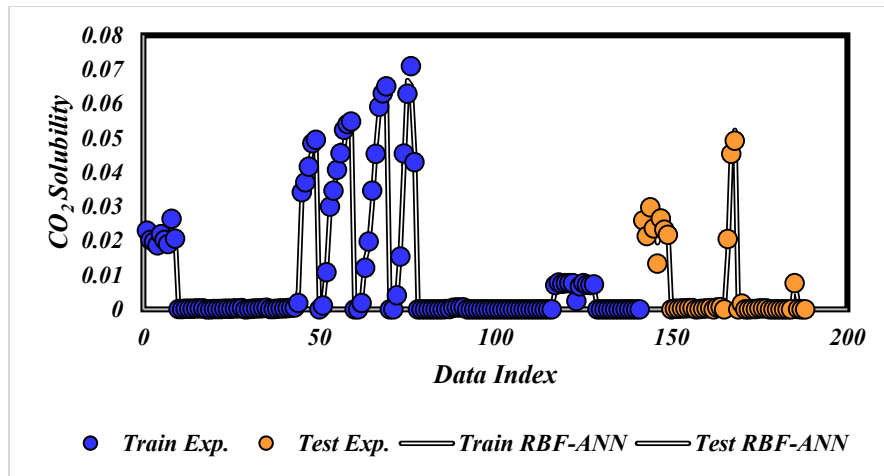
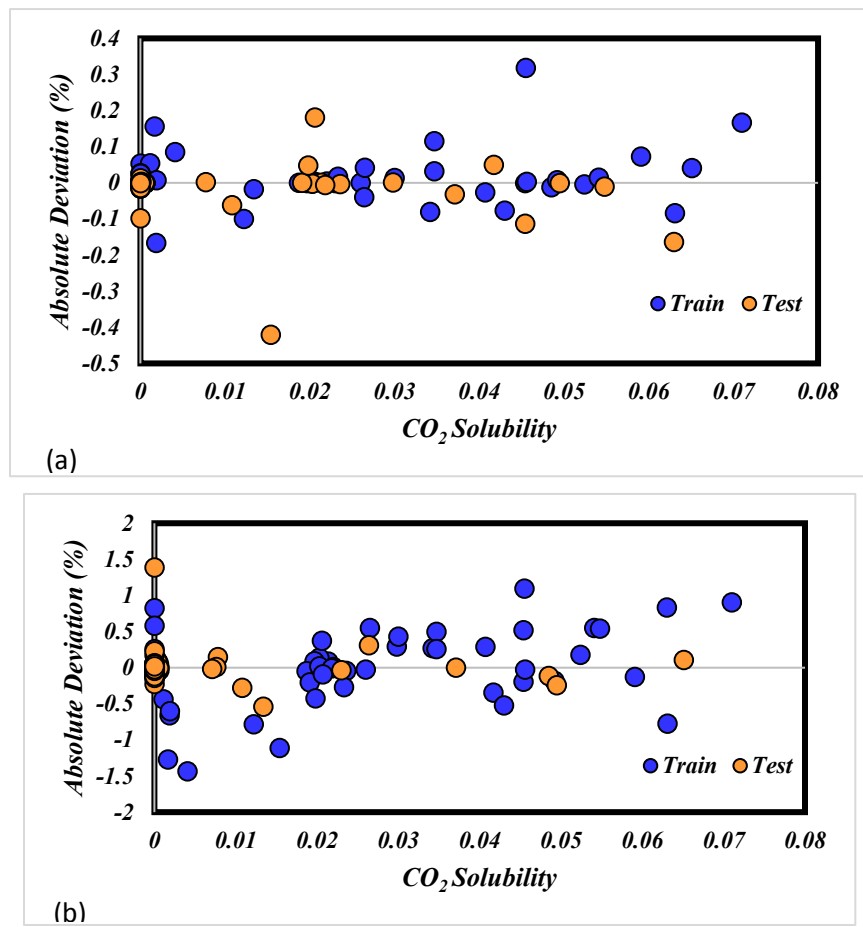**Figure S1:** Experimental and predicted solubility of CO_2 by the proposed models
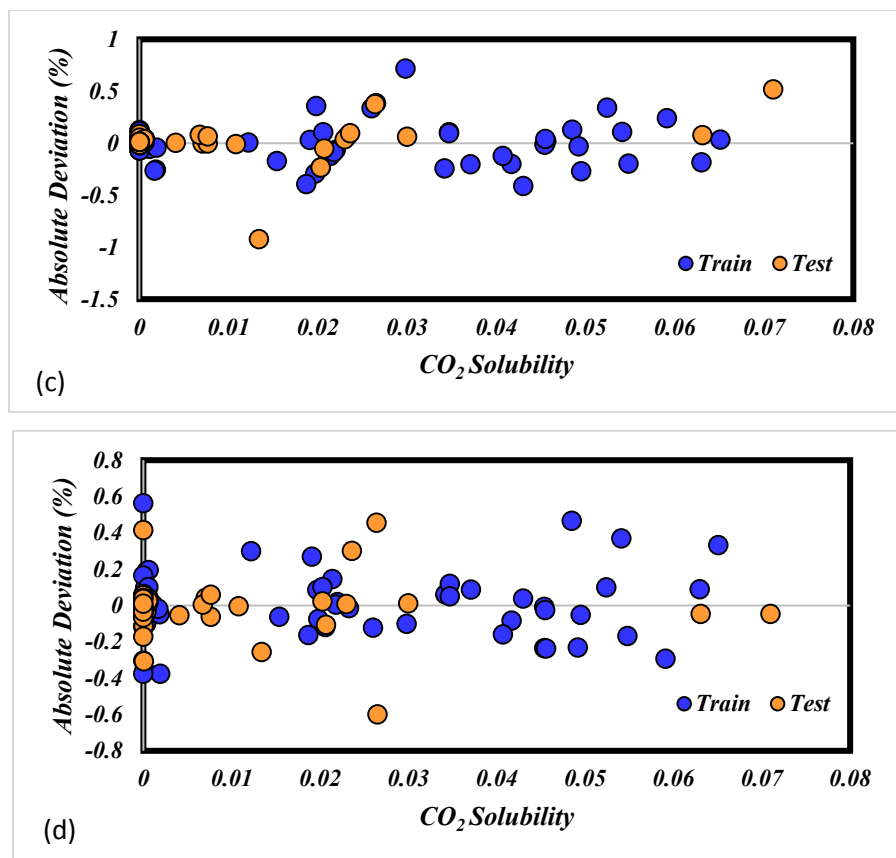

(a)

(b)

Figure S2: Absolut deviation plots for (a) LSSVM, (b) ANFIS, (c) MLP-ANN, and (d) RBF-ANN